derski, *Rev. Geophys. Space Phys.* **18**, 243 (1980).

2. A new observational impetus was given by D. E. Cartwright, A. C. Edden, R. Spencer, J. M. Vassie [*Philos. Trans. R. Soc. London Ser. A* **298**, 87 (1980)] by means of a network of deep-sea bottom-pressure gages. Also encouraging are recent analyses of dissipation by V. Y. Gotlib and B. A. Kagan [*Dtsch. Hydrogr. Z.* **35**, 1 (1982)] and by E. W. Schwiderski (*Mar. Geod.*, in press) from numerical models of M_2.
3. For a recent assessment, see K. Lambeck, *The Earth's Variable Rotation* (Cambridge Univ. Press, New York, 1980, section 10.5).
4. S. S. Hough, *Philos. Trans. R. Soc. London Ser. A* **191**, 139 (1898); M. S. Longuet-Higgins, *ibid.* **262**, 511 (1968).
5. G. W. Platzman, *Science* **178**, 156 (1972); *J. Phys. Oceanogr.* **2**, 117 (1972): *ibid.* **5**, 201 (1975); *ibid.* **8**, 323 (1978); V. Y. Gotlib and B. A. Kagan, *Dokl. Akad. Nauk SSSR* **251**, 710 (1980); G. W. Platzman, G. A. Curtis, K. S. Hansen, R. D. Slater, *J. Phys. Oceanogr.* **11**, 579 (1981); V. Y. Gotlib and B. A. Kagan, *Dtsch. Hydrogr. Z.* **35**, 45 (1982).
6. The only estimate I know is one made by C. J. R. Garrett and W. H. Munk [*Deep-Sea Res.* **18**, 493 (1971)] from the age of the tide. In a model with a single resonant mode they found a spectral density of 0.01. This is not far from the mean of 0.0062 cited in the text or the value of 0.02 for the most energetic contributor to the synthesis of M_2.
7. After discretization, Laplace's tidal equation for a constituent X of frequency ω is $(L' - \omega B)X' = L\bar{X}$. Here $\bar{X}$ is the equilibrium tide, B the inertia matrix, $L = -iA$ the nondissipative tidal operator, and $L' = L + iD$ the dissipative operator, where D is the dissipation matrix. Details of B, A, and D are given in the fourth paper cited in (*5*) above. We seek to approximate X' by a synthesis $\Sigma\, a_k X_k'$ with a small set of the eigenfunctions X_k' of L'. This narrow-band synthesis will not be an exact solution, so a residual remains when it is substituted for X' in the tidal equation. The coefficients a_k are fixed by requiring this residual to be orthogonal to each of the adjoint eigenfunctions Y_k that correspond to the selected X_k'. The well-known result is

$$a_k = (\sigma_k' - \omega)^{-1}\, Y_k^H\, L\, \bar{X} / Y_k^H B\, X_k'$$

If D is small in the sense that σ_k' and X_k' differ only slightly from the nondissipative σ_k and X_k obtained with $D = 0$, then standard perturbation theory leads to $\delta\sigma_k = i\, X_k^H\, D\, X_k$ and

$$\delta X_k = i \sum_{j \neq k} (\sigma_k - \sigma_j)^{-1}\, (X_j^H D\, X_k)\, X_j$$

while $\delta Y_k = \delta X_k$. By this means a dissipative synthesis can be approximated in terms of nondissipative modes.

8. This condition was suggested for tide models by J. Proudman [*Mon. Not. R. Astron. Soc. Geophys. Suppl.* **5**, 23 (1941)]. Its first use in a numerical model was by F. Gohin [*Proc. 7th Conf. Coastal Eng.* **2**, 485 (1961)] for M_2 in the North Atlantic. Y. Accad and C. L. Pekeris [cited in (*1*) above] applied a modified form of it in their model of M_2 and S_2 in the world ocean. Further modifications were examined by V. Y. Gotlib and B. A. Kagan [in (*2*)].
9. Y. Accad and C. L. Pekeris [in (*1*)], M. E. Parke and M. C. Hendershott [in (*1*)], V. Y. Gotlib and B. A. Kagan [in (*2*)], and E. W. Schwiderski [in (*2*)] find, respectively, 2.55, 2.22, 1.89, and 1.86 TW. These values are distinctly lower than the assessment of 3.35 TW by K. Lambeck [in (*3*), section 10.4] from earlier tide models, and point to the long-standing discrepancy between estimates of ocean-tide dissipation and inferences from the observed secular acceleration of the moon.
10. The Q values in recent numerical models of M_2 are: M. E. Parke and M. C. Hendershott [in (*1*)], $Q = 17$ (based on energy equipartition); V. Y. Gotlib and B. A. Kagan [in (*2*)], $Q = 28$ or 29 for three of their parameterizations of dissipation; E. W. Schwiderski [in (*2*)], $Q = 10$. I find the energy of the synthesized M_2 tide partitioned as 56 percent irrotational kinetic, 41 percent potential (in good agreement with Schwiderski's 42 percent), and 3 percent rotational kinetic.
11. W. H. Munk and D. E. Cartwright, *Philos. Trans. R. Soc. London Ser. A* **259**, 533 (1966); see *ibid.*, p. 544.
12. This material is based on work supported by NSF grant OCE-8110929. The manuscript was revised while I was a visitor at the National Center for Atmospheric Research.

22 November 1982; revised 15 February 1983

Phase Transition and Crystal Structure of the 37°C Form of Cholesterol

Abstract. *Crystalline cholesterol undergoes a phase transition a few degrees below human body temperature. The high-temperature form has an unusually complex structure with 16 independent molecules. In the transition two molecules change side chain conformation, four reorient about their long axes, and ten remain unchanged. The transition mechanism implies relatively nonspecific intermolecular interactions, qualitatively consistent with the behavior of cholesterol in biomembranes. The transition preserves a remarkably closely obeyed pseudosymmetry present in the structure.*

The reversible phase transition in crystalline anhydrous cholesterol, first reported in 1965, has been the subject of numerous studies by thermochemical, powder x-ray crystallographic, and nuclear magnetic resonance (NMR) methods (*1–4*). The transition temperature 31.60 ± 0.1°C was determined for single crystals of cholesterol (*3*); the transition enthalpy is 0.69 kcal/mole (*4*). In earlier studies the monohydrate was reported to be the only form present in biological deposits of crystalline cholesterol, such as gallstones and atherosclerotic plaques (*5*). Recently, however, the phase transition was detected in freshly removed human gallstones by means of differential scanning calorimetry (*4*). This indicates that the anhydrous form of cholesterol is present in gallstones in addition to the cholesterol monohydrate, which does not exhibit a transition. A suggested relation between the phase transition and the apparent dependence of atherosclerosis on species body temperature (*6, 7*) remains unsupported in the absence of evidence that the anhydrous form of cholesterol is present in atherosclerotic deposits.

The calorimetric and NMR data have been taken to indicate that the phase transition involves a change in the packing of the side chain methyl groups (*2*) or other rearrangement or onset of disorder in the side chains (*7, 8*). The strong influence of cholesterol content on the gel-liquid crystal phase transitions of lipid bilayers and membranes has been qualitatively ascribed to the lateral packing requirements of rigid steroid skeletons and flexible hydrocarbon chains (*9–12*). To our knowledge, no crystals have yet been prepared of mixed (or stoichiometric, if such exist) phospholipid-cholesterol systems, but the packing of steroid nuclei by themselves and with interdigitating hydrocarbon chains in crystals of cholesterol derivatives has been considered a possible model for biological bilayers (*13*).

Crystals of the body-temperature form grown from 1,4-dioxane solution by slow evaporation at 37°C were mounted, transferred, and examined on the diffractometer while maintained at 37° ± 1°C. Data were collected to a resolution of 0.97 Å (deviation of diffracted beam from direct beam = $2\theta \leq 105°$). The crystals belong to the triclinic space group $P1$ and have a remarkably large unit cell containing 16 independent cholesterol molecules, compared to 8 in the room-temperature (25°C) cell (*14*). The 37°C cell is formed from the 25°C cell by a doubling of the **a** axis. Lattice parameters are given in Table 1.

The structure solution was initiated with an assumed model consisting of two copies of the 25°C structure placed in the 37°C cell and translated by **a**/2 relative to one another. This model was first refined against data for only even values of the index h, using a restrained rigid-body refinement program employing the Gauss-Seidel least-squares algorithm, in which the calculated structure factors are updated after each shift of a rigid group of atoms (*15*). The refinement resulted in considerable rotation of several molecules about their long axes.

Table 1. Comparison of unit cell parameters (*19*) of cholesterol above and below the 31.6°C phase transition.

Temperature (°C)	Unit cell axes (Å)			Unit cell angles (deg)			Z	ρ (g cm^{-3})
	a	**b**	**c**	α	β	γ		
37*	27.565(10)	35.776(16)	10.748(4)	94.45(3)	90.90(3)	73.87(3)	16	1.012
37†	27.565(10)	34.594(15)	10.748(4)	94.25(3)	90.90(3)	96.55(3)	16	1.012
25‡	14.172 (7)	34.209(18)	10.481(5)	94.64(4)	90.67(4)	96.32(4)	8	1.021

*Reduced 37°C cell, whose lattice parameters are related to the reduced 25°C cell by the approximate relations $\mathbf{a}_{37} \simeq 2\mathbf{a}_{25}$, $\mathbf{b}_{37} \simeq \mathbf{a}_{25} + \mathbf{b}_{25}$, and $\mathbf{c}_{37} \simeq \mathbf{c}_{25}$. †Nonstandard 37°C cell, used in Fig. 1, related to the 25°C cell by an approximate doubling of **a**. ‡Reduced 25°C cell (*14*) shown for comparison.

Further refinement against all data, first by restrained-group and ultimately by anisotropic block diagonal methods, gave a value of 0.080 for the agreement index R for the 18,047 measured reflections. The final model included the hydrogen atoms bonded to carbon, in calculated positions.

The 37°C and room-temperature structures (Fig. 1) resemble each other in overall arrangement of molecules, with alternating hydrophobic and hydrophilic layers. The hydrogen bonding pattern is the same in the two structures. In both, the molecules are linked by hydrogen bonds into chains along **c**; these chains form a corrugated sheet parallel to the **ac** plane.

In going from the room-temperature to the body-temperature phase, molecules A1 and E2 turn by 157° about their long molecular axes, while A2 and E1, which in the room-temperature phase are translationally related to A1 and E2, remain

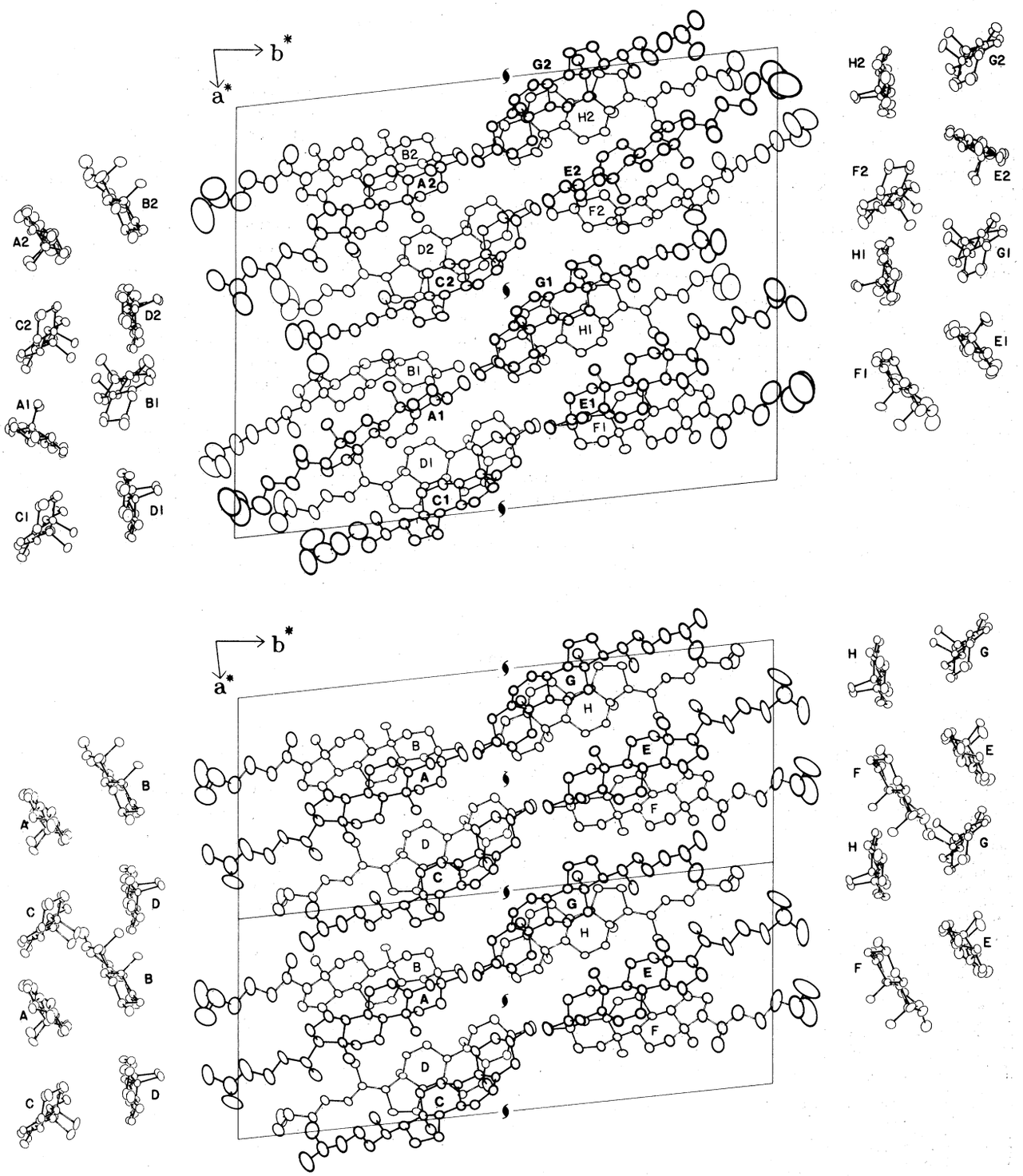

Fig. 1. One unit cell of the 37°C structure (top) compared to two cells of the 25°C structure (bottom). Each middle diagram is a view along the **c** axis. For ease of comparison a nonstandard cell frame is used for the 37°C structure (Table 1). End views of the left (right) half of each structure, with side chains omitted, are shown on the left (right) of the **c**-axis views. Atoms are plotted as 25 percent probability ellipsoids. Symmetry axes shown are noncrystallographic, pseudo-screw axes. Molecules denoted A, . . . , H in the 25°C structure correspond to A1, A2, . . . , H1, H2 in the 37°C form.

essentially unchanged. Similarly, B1 and F2 turn by 87°, while B2 and F1 remain unchanged. The rest of the molecules, including the pairs C, D, G, and H, are essentially unaffected, none exhibiting rotation of the steroid nucleus by more than 4°. There is little change in any of the side chains, except those of C2 and G1, whose conformation changes from *gauche-trans* to the energetically more stable (*16*) *trans-trans* and whose terminal isopropyl groups become disordered.

The mechanism of the transition can be understood by considering intermolecular packing contacts made by the rotated and unrotated molecules and by the side chains of molecules C and G. Molecule C in the room-temperature and C1 in the body-temperature form have the energetically unfavorable *gauche-trans* side chain conformation. This is a consequence of crowding by their neighbor molecules B, notably by the methyl group (C21) at the base of the side chain (Fig. 1). Rotation of B1 allows the side chain of C2 to extend to *trans-trans*. However, the rotated B1 interferes with molecule A in its room-temperature orientation; this interference is, in turn, relieved by the rotation of A1. Of the eight possible combinations for the three molecules:

C: *gauche-trans* (C1) or *trans-trans* (C2)

B: rotated (B1) or unrotated (B2)

A: rotated (A1) or unrotated (A2)

only the two actually present, namely C1, B2, A2 and C2, B1, A1, give acceptable intermolecular packing. It is noteworthy that neither combination interferes with molecule D, which explains why this molecule remains unaffected. By the pseudosymmetry present in the structure (see below), the same mechanism applies to molecules G, F, and E. The ability of molecules to turn about their long axes without disrupting the overall crystalline packing and the multitude of different lateral packing contacts exhibited by the steroid nuclei (Fig. 1, end views) support a biomembrane model involving random, relatively nonspecific lateral interactions (*9*).

Closely obeyed rotational or translational pseudosymmetry exists in the crystal structure of the anhydrous room-temperature form (*14*), as well as in the monohydrate (*17*) and the hemiethanolate (*18*) of cholesterol. The molecular reorientations and the onset of side chain disorder in the phase transition are all related by one set of twofold pseudoscrew axes present in the anhydrous room-temperature form (Fig. 1). The result is that every other axis of pseudosymmetry is preserved in the transition, while every other one is destroyed. The preserved axes are very closely obeyed. A rotation of 180.3° about an axis at the center of the diagram (Fig. 1, top), almost parallel to **c**, accompanied by a translation of approximately **c**/4 superposes the 224 atoms of the left half of the cell (molecules B1, A1, . . . , D2, C2) onto the right half (molecules F2, E2, . . . , H1, G1) with a mean atom-atom misfit of only 0.3 Å, side chains included.

LEH-YEH HSU
C. E. NORDMAN
Department of Chemistry, University of Michigan, Ann Arbor 48109

References and Notes

1. H. L. Spier and K. G. van Senden, *Steroids* **6**, 871 (1976).
2. K. Van Putte, W. Skoda, M. Petroni, *Chem. Phys. Lipids* **2**, 361 (1968).
3. N. N. Petropavlov and N. F. Kostin, *Sov. Phys. Crystallogr.* **21**, 8 (1976).
4. E. Dubler and B. Kamber, in *Thermal Analysis, Proceedings of the 6th International Conference on Thermal Analysis* (Birkhäuser, Basel, 1980), pp. 531–539.
5. H. Bogren and K. Larsson, *Biochim. Biophys. Acta* **75**, 65 (1963); S. S. Katz, G. G. Shipley, D. M. Small, *J. Clin. Invest.* **58**, 200 (1976); D. M. Small and G. G. Shipley, *Science* **185**, 222 (1974); S. S. Katz and D. M. Small, *J. Biol. Chem.* **225**, 9753 (1980).
6. L. C. Labowitz, *Thermochim. Acta* **3**, 419 (1972).
7. N. Garti, L. Karpuj, S. Sarig, *ibid.* **35**, 343 (1980).
8. P. G. Barton, *Chem. Phys. Lipids* **16**, 195 (1976).
9. J. E. Rothman and D. M. Engelman, *Nature (London) New Biol.* **237**, 42 (1972).
10. H.-H. Hinz and J. M. Sturtevant, *J. Mol. Biol.* **247**, 3967 (1972).
11. E. Oldfield and D. Chapman, *FEBS Lett.* **23**, 285 (1972); D. Chapman, *Q. Rev. Biophys.* **8**, 185 (1975).
12. D. J. Recktenwald and H. M. McConnell, *Biochemistry* **20**, 4505 (1981).
13. S. Abrahamsson, B. Dahlén, H. Löfgren, I. Pascher, S. Sundell, in *Structure of Biological Membranes*, S. Abrahamsson and I. Pascher, Eds. (Plenum, New York, 1977), p. 1; B. Dahlén, *Chem. Phys. Lipids* **23**, 179 (1979).
14. H.-S. Shieh, L. G. Hoard, C. E. Nordman, *Nature (London)* **267**, 287 (1977); *Acta Crystallogr. Sect. B* **37**, 1538 (1981).
15. L. G. Hoard and C. E. Nordman, *Acta Crystallogr. Sect. A* **35**, 1010 (1979).
16. W. L. Duax, J. F. Griffin, D. C. Rohrer, C. M. Weeks, *Lipids* **15**, 783 (1980).
17. B. M. Craven, *Nature (London)* **260**, 727 (1976); *Acta Crystallogr. Sect. B* **35**, 1123 (1979).
18. H.-S. Shieh, L. G. Hoard, C. E. Nordman, *ibid.* **38**, 2411 (1982).
19. Symbols: **a**, **b**, and **c** are the unit cell axes; α, β, and γ are the angles between the unit cell edges; Z is the number of molecules per unit cell; and ρ is the density.
20. This work was supported in part by NIH grant GM15259.

12 October 1982; revised 18 January 1983

High-Efficiency Ligation and Recombination of DNA Fragments by Vertebrate Cells

Abstract. *DNA-mediated gene transfer (transfection) is used to introduce specific genes into vertebrate cells. Events soon after transfection were quantitatively analyzed by determining the infectivity of the DNA from an avian retrovirus and of mixtures of subgenomic fragments of this DNA. The limiting step of transfection with two DNA molecules is the uptake by a single cell of both DNA's in a biologically active state. Transfected cells mediate ligation and recombination of physically unlinked DNA's at nearly 100 percent efficiency.*

Studies of stable transformants after specific genes have been introduced into cells have shown that physically unlinked DNA's can be transferred into the same cell and become physically linked to one another (*1*). Studies of DNA soon after transformation show that intramolecular blunt-end ligation is as efficient as intramolecular homologous cohesive-end ligation (*2*) and that the efficiency of intramolecular cohesive-end ligation is approximately 10 percent (*3*).

When two DNA molecules are used in DNA-mediated gene transfer (transfection) experiments, intermolecular ligation and recombination can occur. In studies of transfection with two overlapping SV40 DNA fragments, the infectivity of the two fragments was 0.1 percent (*4*), or 1 percent (*5*) of the infectivity of circular SV40 DNA. After transfection of cells with both SV40 DNA and an unrelated, physically unlinked DNA, recombination occurred in 1 percent of the cells that replicated SV40 DNA (less than 1 percent of all cells) (*6*). The number of cells receiving both DNA's, and thus the efficiency of cell-mediated joining of input DNA's, was not determined.

We have carried out experiments designed to determine the efficiency of cell-mediated joining of DNA's and the limiting step of cotransfection experiments. Our results show that cells physically join unlinked DNA's at close to 100 percent efficiency and that the limiting step of cotransfection is the ability of a single cell to take up both DNA's in a biologically active state.

For cotransfection experiments, we used mixtures of subgenomic DNA clones from spleen necrosis virus (SNV) and looked for production of infectious virus. Spleen necrosis virus is an avian retrovirus that is highly pathogenic in vivo (*7*). In cell culture SNV causes cell death during acute infection (*8*), although some cells survive and multiply while continuing to produce virus (*9*). The introduction of SNV DNA into susceptible